

Shift in metabolic fuel in acylation-stimulating protein-deficient mice following a high-fat diet.

Citation for published version (APA):

Schrauwen, P., Moonen Kornips, E., St Onge, J., Hesselink, M. K., Richard, D., Joanisse, D. R., & Cianflone, K. (2008). Shift in metabolic fuel in acylation-stimulating protein-deficient mice following a high-fat diet. *American Journal of Physiology : Endocrinology and Metabolism*, 294(6), E1015-E1019. <https://doi.org/10.1152/ajpendo.00689.2007>

Document status and date:

Published: 01/01/2008

DOI:

[10.1152/ajpendo.00689.2007](https://doi.org/10.1152/ajpendo.00689.2007)

Document Version:

Publisher's PDF, also known as Version of record

Document license:

Taverne

Please check the document version of this publication:

- A submitted manuscript is the version of the article upon submission and before peer-review. There can be important differences between the submitted version and the official published version of record. People interested in the research are advised to contact the author for the final version of the publication, or visit the DOI to the publisher's website.
- The final author version and the galley proof are versions of the publication after peer review.
- The final published version features the final layout of the paper including the volume, issue and page numbers.

[Link to publication](#)

General rights

Copyright and moral rights for the publications made accessible in the public portal are retained by the authors and/or other copyright owners and it is a condition of accessing publications that users recognise and abide by the legal requirements associated with these rights.

- Users may download and print one copy of any publication from the public portal for the purpose of private study or research.
- You may not further distribute the material or use it for any profit-making activity or commercial gain
- You may freely distribute the URL identifying the publication in the public portal.

If the publication is distributed under the terms of Article 25fa of the Dutch Copyright Act, indicated by the "Taverne" license above, please follow below link for the End User Agreement:

www.umlib.nl/taverne-license

Take down policy

If you believe that this document breaches copyright please contact us at:

repository@maastrichtuniversity.nl

providing details and we will investigate your claim.

Shift in metabolic fuel in acylation-stimulating protein-deficient mice following a high-fat diet

Christian Roy,¹ Sabina Pagliarunga,^{1,2} Alexandre Fisette,¹ Patrick Schrauwen,³ Esther Moonen-Kornips,³ Josée St-Onge,⁴ Matthijs K. Hesselink,⁵ Denis Richard,¹ Denis R. Joannisse,^{1,4} and Katherine Cianflone^{1,2}

¹Centre de Recherche Hôpital Laval, Université Laval, Quebec; ²Department of Biochemistry, McGill University, Montreal, Quebec, Canada; ³Department of Human Biology, Nutrition and Toxicology Research Institute, Maastricht University, Maastricht, The Netherlands; ⁴Division de Kinésiologie, Département de Médecine Sociale et Préventive, Université Laval, Ste-Foy, Quebec, Canada; and ⁵Department of Human Movement Sciences, Nutrition and Toxicology Research Institute, Maastricht University, Maastricht, The Netherlands

Submitted 25 October 2007; accepted in final form 26 March 2008

Roy C, Pagliarunga S, Fisette A, Schrauwen P, Moonen-Kornips E, St-Onge J, Hesselink MK, Richard D, Joannisse DR, Cianflone K. Shift in metabolic fuel in acylation-stimulating protein-deficient mice following a high-fat diet. *Am J Physiol Endocrinol Metab* 294: E1051–E1059, 2008. First published April 8, 2008; doi:10.1152/ajpendo.00689.2007.—ASP-deficient mice (C3 KO) have delayed postprandial TG clearance, are hyperphagic, and display increased energy expenditure. Markers of carbohydrate and fatty acid metabolism in the skeletal muscle and heart were examined to evaluate the mechanism. On a high-fat diet, compared with wild-type mice, C3 KO mice have increased energy expenditure, decreased RQ, lower ex vivo glucose oxidation (−39%, $P = 0.018$), and higher ex vivo fatty acid oxidation (+68%, $P = 0.019$). They have lower muscle glycogen content (−25%, $P < 0.05$) and lower activities for the glycolytic enzymes glycogen phosphorylase (−31%, $P = 0.005$), hexokinase (−43%, $P = 0.007$), phosphofructokinase (−51%, $P < 0.0001$), and GAPDH (−15%, $P = 0.04$). Analysis of mitochondrial enzyme activities revealed that hydroxyacyl-coenzyme A dehydrogenase was higher (+25%, $P = 0.004$) in C3 KO mice. Furthermore, Western blot analysis of muscle revealed significantly higher fatty acid transporter CD36 (+40%, $P = 0.006$) and cytochrome *c* (a marker of mitochondrial content; +69%, $P = 0.034$) levels in C3 KO mice, whereas the activity of AMP kinase was lower (−48%, $P = 0.003$). Overall, these results demonstrate a shift in the metabolic potential of skeletal muscle toward increased fatty acid utilization. Whether this is 1) a consequence of decreased adipose tissue storage with repartitioning toward muscle or 2) a direct result of the absence of ASP interaction with the receptor C5L2 in muscle remains to be determined. However, these in vivo data suggest that ASP inhibition could be a potentially viable approach in correcting muscle metabolic dysfunction in obesity.

muscle metabolism; glycolysis; β -oxidation; C3adesArg

ACYLATION-STIMULATING PROTEIN (ASP) is produced by adipocytes through the alternative complement pathway. C3, factor B, and adipsin associate to generate C3a, and the COOH-terminal arginine of C3a is then cleaved rapidly by carboxypeptidase B to produce ASP (C3adesArg) (reviewed in Ref. 4). ASP interacts with its cell surface receptor, C5L2, resulting in increased nonesterified fatty acid (NEFA) uptake and increased triglyceride synthesis through stimulation of diacylglycerol acyltransferase activity (40). ASP, through its effects on triglyceride synthesis, indirectly stimulates lipopro-

tein lipase activity (11). ASP also increases glucose uptake in a number of cell models, including human adipocytes and L6 myotubes via glucose transporter GLUT4 and GLUT3 (in myotubes) translocation to the cell surface (14, 21, 34). On the other hand, ASP inhibits the action of hormone-sensitive lipase (36), effectively enhancing intracellular triglyceride (TG) accumulation. We have shown previously that ASP-deficient mice [C3 knockout (KO)] are leaner with reduced adipose tissue mass and decreased leptin levels (22). We also observed delayed postprandial TG and NEFA clearance after a fat load in both young and old ASP-deficient mice (23, 24). Furthermore, injection of exogenous ASP in ASP-deficient mice before a fatload normalized the TG and NEFA clearance (39).

Interestingly, despite being leaner, C3 KO mice had a significant increase in food intake, which was counterbalanced by increased oxygen consumption, and elevated muscle fatty acid uptake and oxidation. ASP injection in ASP-deficient mice restored fat partitioning toward a wild-type (WT) profile (39). In addition, we recently showed that mice lacking the ASP receptor C5L2 (C5L2 KO) demonstrated a phenotype similar to ASP-deficient mice with delayed postprandial TG clearance, increased dietary intake, and increased muscle fatty acid oxidation (28). Kalant and colleagues (18, 19) demonstrated that C5L2, a G protein-coupled receptor, is a functional ASP receptor. The relation between ASP and C5L2 was demonstrated through gain-of-function (stable transfection) and loss-of-function (antisense and siRNA) assays, which demonstrated that the presence of C5L2 was essential in mediating ASP function (19). The aim of the present study was to identify the mechanism of increased energy expenditure and fat repartitioning in the C3 KO mice and to evaluate the role of muscle, heart, and brown adipose tissue (BAT) in mediating these effects.

MATERIALS AND METHODS

Mice. C3 KO mice were generously donated by Dr. M. Pekna (29). C3 KO mice were on a C57Bl/6 background and had been backcrossed for at least eight generations, and they were bred in our facility concurrently with WT C57Bl/6 mice. Mice were maintained in a sterile barrier facility under a 12:12-h light-dark cycle and housed individually. At 8 wk, mice were placed on either a standard low-fat (LF) diet (10% kcal from fat; Charles River Laboratories) or a high-fat

Address for reprint requests and other correspondence: K. Cianflone, Centre de Recherche Hôpital Laval, Y-2186, 2725 Chemin Ste-Foy, Québec, Canada, G1V 4G5 (e-mail: katherine.cianflone@crhl.ulaval.ca).

The costs of publication of this article were defrayed in part by the payment of page charges. The article must therefore be hereby marked “advertisement” in accordance with 18 U.S.C. Section 1734 solely to indicate this fact.

(HF) diet (45% kcal from fat; Research Diets, New Brunswick, NJ) for 12 wk. Food intake and body weight were measured every 2 days for 12 wk. For each mouse, cumulative caloric intake per body weight was calculated. Results are expressed as an average for WT and KO mice. Six to eight mice per group were used for food intake, plasma analysis, Western blot, and enzyme activity assays. A second set of mice, seven per group, placed on the HF diet for 3 wk were used for indirect calorimetry experiments and ex vivo tissue assays. A third subset of mice (four C3 KO mice) was used in a pair-feeding study. C3 KO pair-fed mice on the HF diet were food restricted to consume the same amount as WT (3.4 g/day) for 12 wk. All protocols were conducted in accordance with the guidelines of and approved by the Canadian Council on Animal Care and the University Animal Care Committee at Université Laval.

Chemicals. [γ - 32 P]ATP, [14 C(U)]glucose, and [9,10- 3 H(N)]palmitic acid were obtained from PerkinElmer Life Science (Boston, MA), and all other biochemicals were from Sigma-Aldrich (St. Louis, MO) or Roche Diagnostics (Laval, QC, Canada) unless otherwise specified.

Indirect calorimetry. Oxygen consumption ($\dot{V}O_2$), carbon dioxide production ($\dot{V}CO_2$), and the respiratory quotient (RQ) were measured over a 24-h period in an open-circuit system with an S-3A1 oxygen analyzer and a CD-3A carbon dioxide analyzer (both from Applied Electrochemistry, Pittsburgh, PA). $\dot{V}O_2$ and $\dot{V}CO_2$ were calculated as milliliters per minute, and RQ was taken as the quotient of $\dot{V}CO_2/\dot{V}O_2$.

Plasma assays and glucose tolerance test. Overnight-fasted 18-wk-old mice were injected intraperitoneally with glucose (2 mg/g body wt in 200 μ l of sterile solution). Blood samples were taken at 0, 30, 60, and 120 min after the injection by tail vein bleeding. Samples were collected in 2% EDTA, and plasma was separated by centrifugation at 5,000 g for 5 min and stored at -20°C . Plasma glucose was measured using a glucose Trinder assay (Sigma). At the time the mice were killed, fasting blood samples were taken by cardiac puncture. Muscle, heart, and brown fat were excised from the mice, weighed, and immediately placed in liquid nitrogen and stored at -80°C until further use. Insulin, leptin, and adiponectin were measured using commercially available RIA kits from Linco (St. Charles, MO). Plasma TG and NEFA were measured using enzymatic colorimetric kits from Roche Diagnostics (Indianapolis, IN) and Wako Chemical (Richmond, VA), respectively.

Skeletal muscle and heart glucose and fatty acid oxidation. [14 C]glucose oxidation was measured by capturing $^{14}\text{CO}_2$ secreted into the medium as described previously, with some modification (10). Briefly, skeletal muscle (quadriceps) and heart were collected after the mice were killed and placed in room-temperature PBS. The tissue was cut into small pieces (10–20 mg) and placed into a glass culture tube with Ca^{2+} -free Krebs-Ringer buffer (500 μ l) containing 1% BSA and 5 mM glucose [^{14}C (U)]glucose, 1 mCi/ml. A piece of filter paper was hung vertically above the reaction solution and fixed to a rubber stopper. The tubes were capped and incubated for 2 h at 37°C . Following the incubation, the filter paper was saturated with a base (CO_2 trapping agent), and 200 μ l of 4 M H_2SO_4 was injected into the medium of each tube (not touching the saturation paper). The tubes were then incubated for an additional 1 h at 37°C with gentle shaking to release $^{14}\text{CO}_2$. The filter papers with captured $^{14}\text{CO}_2$ were transferred to scintillation tubes and counted. The remaining media were carefully removed, and 0.3 N NaOH was added to the tissue to dissolve proteins. Proteins were measured by Bradford method (Bio-Rad, Mississauga, ON, Canada), and results are expressed as picomoles per milligram of protein. Fatty acid oxidation was measured using radiolabeled palmitate as described previously (28).

Western blot. Frozen quadriceps muscle was homogenized in lysis buffer (1 mM EDTA, 0.4 mM phenylmethylsulfonyl fluoride in PBS), SDS gel sample buffer was added, and protein homogenates were separated by electrophoresis on a 12% acrylamide-bis gel at 200 V for 45 min. Proteins were transferred via electroblotting (60 min at 100 V) onto a nitrocellulose membrane. Peroxisome proliferator-

activated receptor- β (PPAR β) and mitochondrial transcription factor A (mtTFA) were visualized with the Odyssey (LI-COR Biotechnology, Lincoln, NE) imaging system. Primary antibody PPAR β sc-7197 rabbit polyclonal (Santa Cruz Biotechnology, Santa Cruz, CA) and secondary donkey anti-rabbit IR800 (Rockland Immunochemicals, Gilbertsville, PA) and primary mtTFA sc-19050 goat polyclonal (Santa Cruz) and secondary donkey anti-goat Alexa 680 (Molecular Probes, Eugene, OR) were used for detecting PPAR β and mtTFA, respectively. For the evaluation of CD36, cytochrome *c* content, and uncoupling protein 3 (UCP3), blocking, antibody incubation, and visualization procedures were followed as previously described by Pagliarunga et al. (28).

Quadriceps muscle and heart metabolic enzyme activity assays. Muscles were maintained frozen at -80°C until assayed for maximal (V_{max}) enzyme activities. The muscle samples were pulverized into powder to avoid possible variability caused by fiber-type distribution. Approximately 10 mg of muscle powder was homogenized (1:40 wt/vol for quadriceps, 1:80 wt/vol for heart) with a glass-on-glass Dual homogenizer with ice-cold buffer (0.1 M phosphate buffer, 2 mM EDTA, 1 mM PMSF, pH 7.2). The homogenate was transferred into 1.5-ml polypropylene microtubes and sonicated six times for 5 s at 20 W, on ice, with pauses of 85 s between pulses. Activities of the following enzymes were measured as described previously in detail (8, 12). Potential for glycogenolysis was assessed as the activity of glycogen phosphorylase (PHOS). For glycolysis, hexokinase (HK) and phosphofructokinase (PFK) were measured, as was hydroxyacyl-CoA dehydrogenase (HADH) for fatty acid β -oxidation. For assessment of high-energy phosphate metabolism, citric acid cycle, and evaluation of the respiratory chain potentials, creatine kinase (CK), citrate synthase (CS), and cytochrome *c* oxidase (COX), respectively, were measured. For carnitine palmitoyltransferase I (CPT I), the sonicated homogenate was used for spectrophotometric determination of CPT I by following the appearance of CoASH at 412 nm as described previously (8, 12). Enzyme activities are expressed as micromoles of substrate consumed per minute per gram of wet tissue ($\mu\text{mol}\cdot\text{min}^{-1}\cdot\text{g}^{-1}$). The ratios of PFK to CS, PFK to HADH, and PFK to COX were used as indicators of the relative capacity for glycolytic to aerobic metabolism. Glycogen content was measured with a spectrophotometer as described previously (16).

Quadriceps muscle and cardiac muscle AMP-activated protein kinase activity assay. The AMP-activated protein kinase (AMPK) activity protocol as published by Sambandam et al. (33) was modified as described previously by Pagliarunga et al. (28). Briefly, 20 mg of frozen skeletal muscle (quadriceps) was homogenized for 30 s in 200 μ l of homogenization buffer [50 mM Tris-HCl, pH 8, 1 mM EDTA, 10% (wt/vol) glycerol, 0.02% (vol/vol) Brij-35, 1 mM dithiothreitol] with protease and phosphatase inhibitors. The homogenate was centrifuged at 10 000 g for 20 min at 4°C , and protein content was measured using the Bradford assay (Bio-Rad). AMPK activity was measured by following the incorporation of [γ - 32 P] into the synthetic peptide AMARA {final volume 25 μ l, containing 80 mM HEPES-NaOH, pH 7.0, 160 mM NaCl, 16% glycerol, 1.6 mM EDTA, 200 μ M AMARA peptide, 1 mM MgCl_2 , 2 mM [γ - 32 P]ATP (400–600 dpm/pmol), and 5 μ g of protein homogenate; AMARAASAAALARRR; Upstate, Billerica, MA}. The assay was performed in the absence (for nonspecific background) or presence of AMARA at 30°C for 15 min. Following incubation, 10- μ l aliquots were spotted on P81 phosphocellulose paper (Whatman, Florham Park, NJ), washed with 1% H_3PO_4 , and counted with 5 ml of scintillation fluid.

Statistical analysis. Results are presented as means \pm SE, except for food intake data, which are presented as means \pm SD. Groups were compared with two-way repeated-measures ANOVA, ANOVA, and Student's *t*-test as appropriate. Statistical significance was set as $P < 0.05$.

RESULTS

We first measured food intake relative to body weight over a 10-wk period in C3 KO and WT mice. The C3 KO mice, compared with the WT counterparts, had a 59% increase ($P < 0.0001$) on the LF diet (Fig. 1A) and a dramatic 229% increase ($P < 0.0001$) on the HF diet (Fig. 1B) in cumulative food intake. Interestingly, there was no difference in body weight between WT and C3 KO on either diet during the 10 wk of the experiment, as shown in Table 1. It was shown previously that increased physical activity or changes in body temperature could not adequately explain this imbalance between food intake and body weight observed in C3 KO mice on the LF diet (39). In the present study, C3 KO and WT mice were placed in a metabolic chamber to measure indirect calorimetry after 2 wk on the HF diet. The C3 KO mice displayed a higher $\dot{V}O_2$ consumption than the WT mice, indicating elevated energy expenditure ($P < 0.0001$; Fig. 1C). Also, the C3 KO mice showed a lower RQ compared with their WT counterparts ($P = 0.0017$; Fig. 1D). Taken together, these results imply a difference in energy expenditure and preference for dietary fat as an energy substrate, which was then related to the metabolic machinery of various target tissues, including BAT, skeletal muscle, and cardiac muscle.

Plasma analysis and brown fat. BAT mass was measured following 12 wk on a LF or HF diet. At the time the mice were killed, no significant differences in BAT weight between WT and C3 KO mice on either diet were observed (data not shown). Fasting plasma values were measured for the four groups of mice (Table 1). Levels of insulin, leptin, and adiponectin, hormones known to influence energy storage, food intake, and energy expenditure, were not different when the C3 KO mice were compared with the WT mice under the same diet (Table 1). On the LF diet only, the plasma TG levels were significantly higher in the C3 KO mice. Interestingly, on the

Table 1. Body weight and fasting plasma values of WT and C3 KO mice on LF and HF diets

	WT LF	C3 KO LF	WT HF	C3 KO HF
Body weight, g	30.9 \pm 0.6	32.7 \pm 1.8	38.1 \pm 1.1	40.4 \pm 1.4
Leptin, ng/ml	5.89 \pm 0.92	8.58 \pm 1.83	15.54 \pm 3.93	22.97 \pm 4.92
Adiponectin, μ g/ml	12.32 \pm 1.86	6.64 \pm 1.19	13.88 \pm 2.11	13.13 \pm 2.72
Insulin, ng/ml	0.28 \pm 0.06	0.35 \pm 0.08	0.45 \pm 0.09	0.68 \pm 0.22
TG, mmol/l	0.23 \pm 0.05	0.41 \pm 0.05*	0.25 \pm 0.06	0.58 \pm 0.06†
NEFA, mmol/l	0.63 \pm 0.06	0.82 \pm 0.16	0.57 \pm 0.07	1.17 \pm 0.23*
Glucose, mmol/l	5.82 \pm 0.15	6.13 \pm 0.40	5.41 \pm 0.32	7.72 \pm .77*

Results are expressed as means \pm SE for 6–8 mice. WT, wild type; C3 KO, acylation protein-deficient mice; LF, low fat; HF, high fat; TG, triglycerides; NEFA, nonesterified fatty acids. Statistical significance was evaluated by 2-way ANOVA comparing WT vs. KO, where * $P < 0.01$ and † $P < 0.001$.

HF diet, fasting plasma TG, NEFA, and glucose were elevated in C3 KO compared with WT mice ($P < 0.05$).

Glucose uptake and glycogen stores in skeletal muscle. To evaluate the implication of elevated plasma glucose observed in C3 KO on a HF diet, glucose handling, glycogen content, and variations in maximal activities of key skeletal muscle glycolytic enzymes were measured in the quadriceps muscles of WT and C3 KO mice following LF or HF diets.

Following the HF diet, the C3 KO mice showed a slight, but not significant, delay in glucose clearance compared with controls (data not shown). Several changes in ex vivo glucose metabolism were found in the C3 KO vs. the WT mice on the HF diet. First, C3 KO mice showed lower ex vivo glucose oxidation in quadriceps muscle ($P = 0.018$; Fig. 2A). Second, the C3 KO mice had a 25% decrease in skeletal muscle glycogen content ($P < 0.01$; Fig. 2B). Last, the C3 KO mice showed significantly lower maximal activities for key enzymes of glucose and glycogen utilization. There was a 31% decrease in PHOS activity ($P = 0.005$; Fig. 2C), a key enzyme for

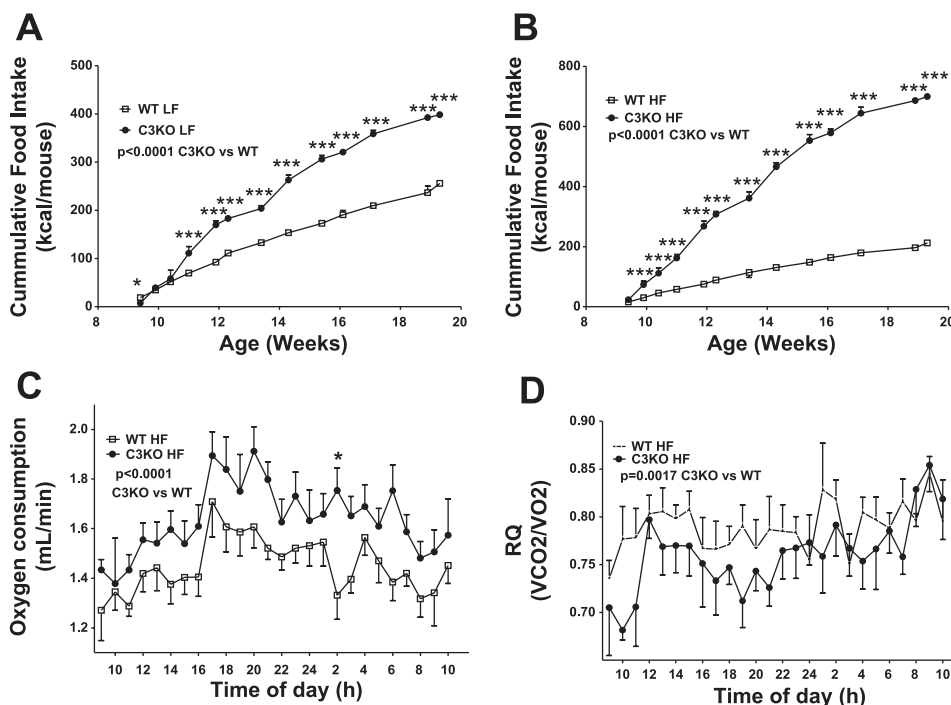


Fig. 1. Increased food intake, energy expenditure, and lower respiratory quotient (RQ) in acylation-stimulating protein (ASP)-deficient (C3 KO) mice. Food intake is increased without changes in body weight in C3 KO mice vs. wild-type (WT) mice on a low-fat (LF) diet (A) and on a high-fat (HF) diet (B). Food intake was measured 2–3 times weekly and was assessed for each mouse individually. Food intake (means \pm SD) is expressed as kcal consumed/mouse. Cumulative food intake was measured over a 10-wk period for WT mice (\square) and C3 KO mice (\bullet); $n = 6$ –8 mice/group. Oxygen consumption and RQ were measured following 2 wk on a HF diet. C3 KO mice have an elevated oxygen consumption ($\dot{V}O_2$; C) and a lower RQ (D). $\dot{V}O_2$, carbon dioxide production ($\dot{V}CO_2$), and RQ were measured over 24 h. Results are expressed as means \pm SE for WT mice (\square) and C3 KO mice (\bullet); $n = 6$ –8 mice/group. Significance was determined by 2-way repeated-measures ANOVA, where * $P < 0.05$ and **** $P < 0.0001$.

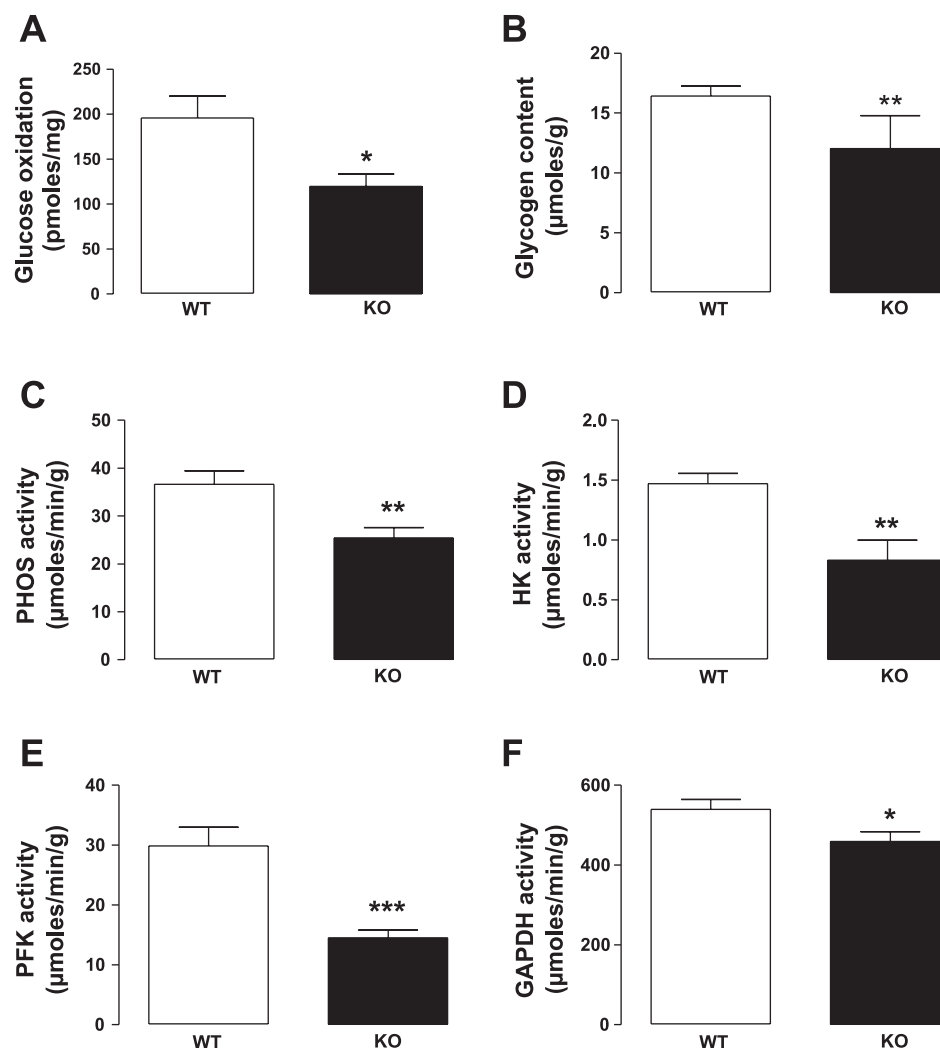


Fig. 2. C3 KO mice on a HF diet have decreased skeletal muscle ex vivo glucose oxidation and a reduced potential for glycolysis, as assessed by ex vivo glucose oxidation (A), muscle glycogen content (B), and glycogen phosphorylase (PHOS; C), hexokinase (HK; D), phosphofructokinase (PFK; E), and glyceraldehyde-3-phosphate dehydrogenase (GAPDH; F) activities. Ex vivo glucose oxidation was measured in quadriceps muscle pieces, whereas enzyme activities were assessed in quadriceps muscle homogenates derived from WT (open bars) and C3 KO (black bars) mice on a HF diet. Results are expressed as means \pm SE for 6–8 mice/group, where * P < 0.05, ** P < 0.01, and *** P < 0.001.

breakdown of glycogen to glucose. HK activity, which regulates glucose phosphorylation for entry into glycolysis, was decreased by 45% (P = 0.007; Fig. 2D). Furthermore, a 51% decrease in PFK activity, the rate-limiting enzyme for glycolysis (P < 0.0001; Fig. 2E), was also demonstrated. Glyceraldehyde-3-phosphate dehydrogenase (GAPDH) activity, an enzyme controlling glucose entry into the citric acid cycle, was decreased by 15% (P = 0.04; Fig. 2F).

On the LF diet, C3 KO mice maintained fasting glucose levels comparable with WT mice (Table 1), yet they showed a significantly delayed glucose clearance (incremental area under the curve for WT LF: 11.9 ± 2.6 mmol \cdot l $^{-1}\cdot$ min $^{-1}$, and C3 KO LF: 20.4 ± 1.4 mmol \cdot l $^{-1}\cdot$ min $^{-1}$, P = 0.017), a 49% decrease in muscle glycogen content (P = 0.009; Table 2), and a significantly higher PFK activity compared with their WT counterparts.

Fatty acid handling in the skeletal muscle. In addition to glucose oxidation, palmitate metabolism was also evaluated in the quadriceps muscle. In relation to the WT mice, ex vivo fatty acid oxidation in the C3 KO mice was significantly increased (P = 0.019; Fig. 3A). Proteins involved in fatty acid channelling in the skeletal muscle were also evaluated. We observed 40% more skeletal muscle CD36 protein content, a key membrane fatty acid transporter, in the C3 KO mice

relative to the WT mice on the HF diet (P = 0.006; Fig. 3B). The activity of CPT I, the rate-limiting step of fatty acid entry into mitochondria, was also assayed. As shown in Fig. 3C, no significant difference was detected between the WT and C3 KO mice on a HF diet. No change was detected in UCP3 (see results below). No significant differences were observed on the LF diet for either CD36 or CPT I (Table 2).

Mitochondrial enzyme activities and proteins in skeletal muscle. A number of mitochondrial enzyme activities were assayed. Results showed a 25% increase in HADH activity, a key enzyme in β -oxidation (P = 0.004; Fig. 4A), and a 69% increase in cytochrome *c* content, which is indicative of cellular mitochondrial content (P = 0.034; Fig. 4B) in C3 KO mice compared with the WT mice on the HF diet. Interestingly, there were also greater activities of two mitochondrial enzymes assayed in the mice muscle from animals on the LF diet; C3 KO mice presented a 42% increase in HADH (Table 2) and a 43% increase in CS activity compared with the WT mice (P = 0.025; Table 2). The cytochrome *c* upregulation indicates that the mitochondrial biogenesis pathway could be affected. To clarify this, we assessed mtTFA and PPAR β protein content via Western blot. There was no significant change in mtTFA or PPAR β content between the C3 KO mice and their WT counterparts (Fig. 6D), indicating that increased mitochondrial

Table 2. Markers of glycolysis, fatty acid oxidation, and energy metabolism in skeletal muscle of C3 KO and WT mice on the LF diet

	WT	C3 KO
Glycogen, $\mu\text{mol/g}$	34.19 ± 3.02	$17.48 \pm 3.88^\dagger$
PHOS, $\mu\text{mol} \cdot \text{min}^{-1} \cdot \text{g}^{-1}$	29.19 ± 2.70	26.10 ± 1.26
HK, $\mu\text{mol} \cdot \text{min}^{-1} \cdot \text{g}^{-1}$	1.23 ± 0.16	1.13 ± 0.12
PFK, $\mu\text{mol} \cdot \text{min}^{-1} \cdot \text{g}^{-1}$	17.00 ± 2.03	$25.69 \pm 2.50^*$
GAPDH, $\mu\text{mol} \cdot \text{min}^{-1} \cdot \text{g}^{-1}$	438.0 ± 33.5	466.1 ± 24.1
CD36, arbitrary units	86.04 ± 6.56	66.08 ± 10.03
CPT I, $\mu\text{mol} \cdot \text{min}^{-1} \cdot \text{g}^{-1}$	0.130 ± 0.005	0.156 ± 0.015
HADH, $\mu\text{mol} \cdot \text{min}^{-1} \cdot \text{g}^{-1}$	9.98 ± 1.43	$14.12 \pm 0.68^*$
Cyto c, % of WT LF	100.0 ± 37.05	70.12 ± 29.56
CS, $\mu\text{mol} \cdot \text{min}^{-1} \cdot \text{g}^{-1}$	9.59 ± 0.98	$13.74 \pm 1.33^*$
AMPK, $\text{nmol} \cdot \text{min}^{-1} \cdot \text{g}^{-1}$	0.037 ± 0.007	0.046 ± 0.006
CK, $\mu\text{mol} \cdot \text{min}^{-1} \cdot \text{g}^{-1}$	661.0 ± 50.3	569.3 ± 21.8
COX, $\mu\text{mol} \cdot \text{min}^{-1} \cdot \text{g}^{-1}$	3.04 ± 0.36	3.84 ± 0.41
Heart AMPK, $\text{nmol} \cdot \text{min}^{-1} \cdot \text{g}^{-1}$	0.08 ± 0.01	0.04 ± 0.005

Results are expressed as means \pm SE for 6–8 mice. PHOS, glycogen phosphorylase; HK, hexokinase; PFK, phosphofructokinase; CPT I, carnitine palmitoyltransferase I; HADH, hydroxyacyl-CoA dehydrogenase; Cyto c, cytochrome c; CS, citrate synthase; AMPK, AMP-activated protein kinase; CK, creatine kinase; COX, cytochrome c oxidase. Significance was determined by *t*-test comparing WT vs. KO, where $^*P < 0.05$ and $^\dagger P < 0.01$.

biogenesis was not the major mechanism for the increase in mitochondrial activity.

The ratio of key enzymes involved in fuel utilization was used as an indicator of the relative maximal potential of different metabolic pathways within the muscle. The ratio of PFK activity (the rate-limiting enzyme in glycolysis) to HADH, CS, and cytochrome oxidase activities is reported in Table 3. C3 KO mice on the HF diet show a significant decrease in the PFK/HADH ratio (Fig. 4C). The ratios shown in Table 3 report an overall, but nonsignificant, decrease in PFK/CS and PFK/COX in C3 KO mice on the HF diet.

Muscle fuel metabolism. Skeletal muscle assays revealed significantly lower activities of two enzymes involved in the energy metabolism in the C3 KO mice. On the HF diet, AMPK activity was reduced by 48% ($P = 0.003$; Fig. 5A) in the C3 KO mice compared with the WT mice. Also, on the same diet, we observed a 45% decrease in CK maximal activity in the C3 KO mice ($P < 0.0001$; Fig. 5B). Interestingly, this decrease in enzyme activity was specific to C3 KO mice on the HF diet, as there were no significant differences between C3 KO and WT mice on the LF diet (Table 2).

Studies on pair-fed mice. A subset of C3 KO mice were pair-fed a HF diet for 12 wk matched to the food intake of their WT counterparts, thereby controlling for the hyperphagia of the C3 KO mice. As shown in Fig. 6A, the pair-fed C3 KO mice had a lower body weight than the WT mice. Compared with their WT counterparts, the pair-fed C3 KO mice displayed significantly lower levels of plasma insulin and adiponectin (Fig. 6, B and C). They also had higher UCP3 and cytochrome c protein levels as assayed by Western Blot (Fig. 6D).

Cardiac muscle. In our previous and present studies, C3 KO mice did not display any obvious functional or morphological changes in cardiac muscle such as heart size, lipid deposits, or sudden death (Roy C, personal observations). In the present study, heart (cardiac) tissue was evaluated to determine any similarities with the skeletal muscle for the modified substrate utilization documented above. Cardiac muscle was used to

evaluate ex vivo oxidation and maximal activities for key regulators of glucose and fatty acid oxidation on a HF diet. Although there were significant differences between C3 KO and WT mice in skeletal muscle for both substrate oxidations, there was no difference in ex vivo glucose oxidation in cardiac tissue (Fig. 7A), but there was a significant increase in ex vivo fatty acid oxidation ($P = 0.04$; Fig. 7B). On the HF diet, C3 KO mice displayed significant changes in enzyme activities (Fig. 7). Similar to skeletal muscle, in C3 KO mice on the HF diet, cardiac CK activity was decreased by 42% ($P = 0.036$; Fig. 7C) and AMPK activity was decreased by 45% ($P = 0.025$; Fig. 7D). CPT I activity was decreased by 46% ($P = 0.008$; Fig. 7E), and GAPDH activity was increased by 45% ($P = 0.010$; Fig. 7F). However, there were no changes in the maximal activities of the following enzymes: PHOS, PFK, HADH, and CS. Interestingly, on the LF diet, C3 KO cardiac AMPK activity was also significantly lower than in WT mice ($P = 0.0006$; Fig. 7D).

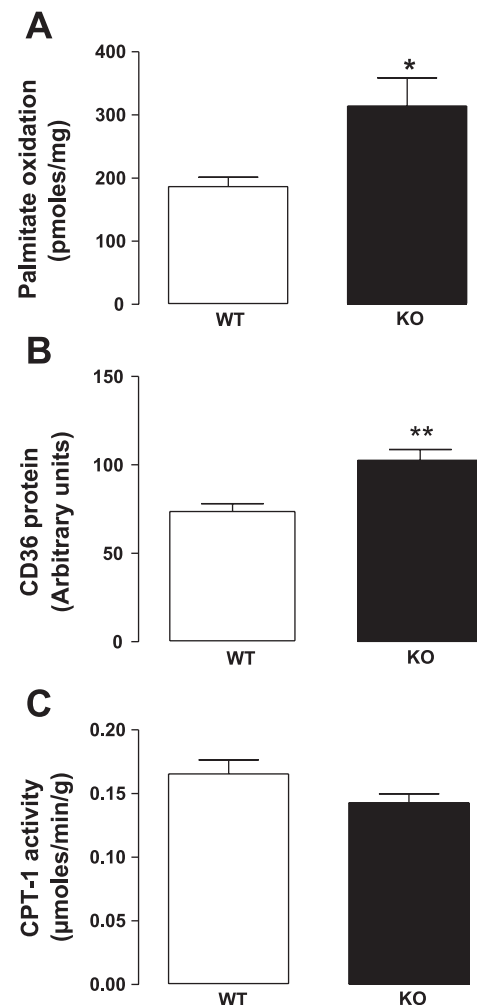


Fig. 3. C3 KO mice on HF diet have increased ex vivo palmitate oxidation and greater CD36 content in skeletal muscle. A: ex vivo fatty acid palmitate oxidation is increased in C3 KO mice, as measured in quadriceps muscle of C3 KO and WT mice. CD36 content (B) was evaluated by Western blot, and carnitine palmitoyltransferase I (CPT I) maximal activity (C) was assessed in muscle homogenates. All results are expressed as means \pm SE in WT mice (open bars) and C3 KO mice (black bars) on the HF diet for $n = 6$ –8 mice/group, where $^*P < 0.05$ and $^{**}P < 0.01$.

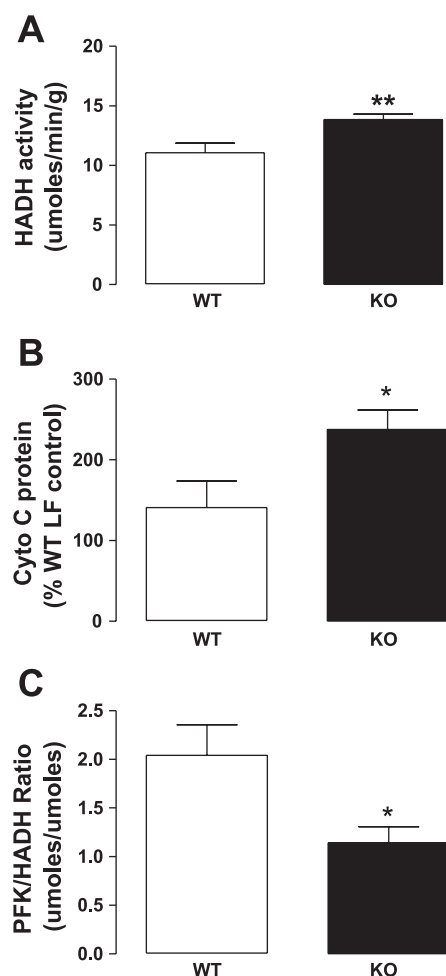


Fig. 4. Increased potential for mitochondrial metabolism in skeletal muscle of C3 KO mice on a HF diet. *A*: C3 KO mice on HF diet had increased hydroxyacyl-CoA dehydrogenase (HADH) maximal activity. *B*: C3 KO mice also demonstrated increased cytochrome *c* content. *C*: the switch in the potential for metabolic fuel utilization in C3 KO mice is indicated by the decrease in ratio of PFK/HADH activities. Results are expressed as means \pm SE; $n = 6-8$ mice in each case, where $*P < 0.05$ and $**P < 0.01$.

DISCUSSION

C3 KO mice, on either a LF or HF diet, demonstrated higher food intake while maintaining similar body weight to WT mice. Interestingly, these results were not associated with significant differences in leptin, insulin, or adiponectin levels, hormones known to influence energy metabolism, suggesting a process directly related to the absence of ASP. Furthermore, in BAT, a source of energy expenditure through UCPs (3), no

Table 3. Relative potential for pathways of energy metabolism expressed as ratios of enzymes involved in glucose and fatty acid oxidation in skeletal muscle

Ratios	WT LF	C3 KO LF	WT HF	C3 KO HF
PFK/CS	1.72 \pm 0.36	1.94 \pm 0.29	2.32 \pm 0.50	1.44 \pm 0.35
PFK/HADH	2.06 \pm 0.45	1.94 \pm 0.30	2.04 \pm 0.31	1.14 \pm 0.17*
PFK/COX	5.97 \pm 0.86	7.02 \pm 0.83	9.43 \pm 2.11	6.28 \pm 1.94

Results are expressed as means \pm SE (in μ mol) for 6–8 mice, where significance was determined by *t*-test comparing WT vs. KO, where $*P < 0.05$.

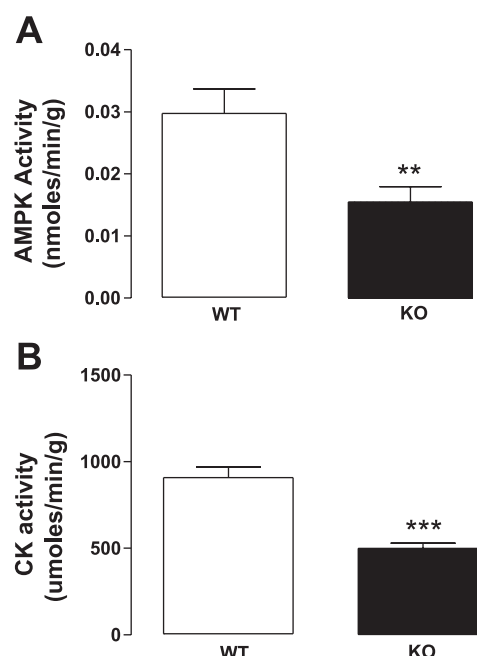


Fig. 5. Decreased AMP kinase (AMPK) and creatine kinase (CK) activities in C3 KO mice on a HF diet. *A*: C3 KO mice have decreased maximal AMPK activity. *B*: for the same diet, CK activity is also decreased in the C3 KO. Results are expressed as means \pm SE; $n = 6-8$ mice in each group, where $**P < 0.01$ and $***P < 0.001$.

differences were observed in BAT weight, and we previously reported downregulation of UCP1 (39). This implies that the imbalance in caloric intake between the C3 KO and the WT mice is controlled by a mechanism unrelated to BAT activation.

Skeletal muscle represents $\sim 38\%$ of total body weight in both mice and humans (2) and plays an important role in fuel storage and utilization. In the present study, we observed a rearrangement of the metabolic machinery that favors fatty acid oxidation in C3 KO mice skeletal muscle. This was seen under both diets but was more pronounced in the HF diet. On the LF diet, differences in substrate use were demonstrated by delayed glucose clearance, lower muscle glycogen content, and increased HADH and citrate synthase activities in the quadriceps muscle. On the HF diet, the ASP-deficient mice showed a similar shift in metabolic potential toward fatty acid oxidation in the quadriceps muscle. This was demonstrated by a lower RQ, lower ex vivo glucose oxidation, higher ex vivo fatty acid oxidation, and lower muscle glycogen content. In addition, the maximal activities of four key glycolytic enzymes (PHOS, HK, PFK, and GAPDH) decreased, whereas HADH activity increased, as did CD36 and cytochrome *c* content in C3 KO mice. Last, the lower PFK/HADH ratio further supports the shift in metabolic potential from glucose oxidation toward lipid utilization (13). However, these differences appear to be mediated through both increased mitochondrial activity and content.

In our previous studies on the ASP-C5L2 pathway, we found that the C3 KO mice had increased food intake, delayed postprandial TG clearance, elevated oxygen consumption and increased fatty acid uptake, and oxidation in muscle after a fat load (24, 25, 39). Similar results were recently obtained in C5L2 KO mice, which are ASP receptor-deficient mice (28).

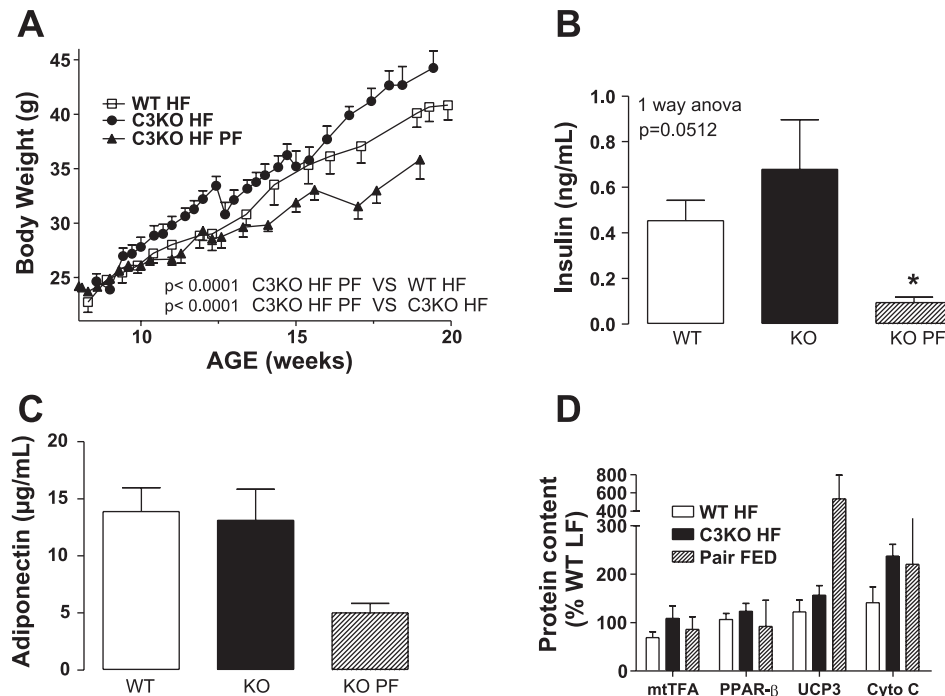


Fig. 6. Controlled food intake leads to decreased body weight, insulin level, and adiponectin level in C3 KO mice. A: studies on pair-fed mice show that C3 KO mice with food intake maintained at the level of WT mice have a lower body weight. Body weight was measured over a 12-wk period for WT mice (\square), C3 KO mice (\bullet), and C3 KO pair-fed (PF) mice (\blacktriangle), where $P < 0.0001$ by linear regression analysis between PF C3 KO and WT mice. Plasma levels of insulin (B) and adiponectin (C) were lower in PF C3 KO mice vs. WT. D: protein levels of mitochondrial transcription factor A (mtTFA), peroxisome proliferator-activated receptor- β (PPAR β), uncoupling protein 3 (UCP3), and cytochrome *c* (Cyto *c*) were assayed by Western blot. PF C3 KO mice showed increased UCP3 and cytochrome *c*. Results are expressed as means \pm SE; $n = 4-8$ mice in each case, where $*P < 0.05$.

The influence of the ASP-C5L2 pathway on energy expenditure was also evaluated in double-knockout leptin-deficient *ob/ob* and ASP-deficient mice. Strikingly, the lack of ASP in *ob/ob* mice reduced weight gain, improved insulin sensitivity, and increased energy expenditure (38). The imbalance be-

tween energy intake and energy expenditure could not be explained by increased physical activity or obvious changes in body temperature; however, the data were consistent with increased muscle fatty acid metabolism (38). Altogether, the previous studies support the hypothesis that mice lacking

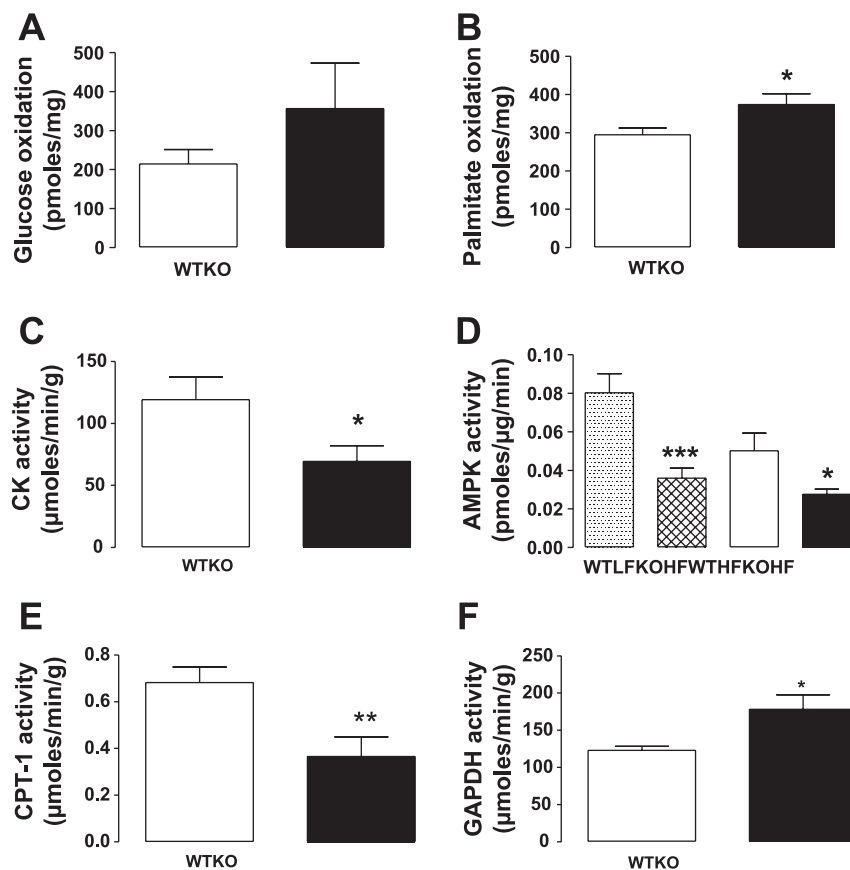


Fig. 7. Cardiac muscle ex vivo oxidation and maximal enzyme activities in C3 KO mice on a HF diet. Ex vivo glucose (A) and fatty acid palmitate (B) oxidation were measured in heart tissue. No significant changes were present in glucose oxidation for the C3 KO mice, whereas an increase in fatty acid palmitate oxidation was observed in these mice. Cardiac muscle from C3 KO mice demonstrated decreased CK (C), AMPK (D), and CPT I (E) maximal activities. GAPDH activity (F) was increased in the C3 KO mice on the HF diet. Results are expressed as means \pm SE; $n = 6-8$ mice in each case, where $*P < 0.05$, $**P < 0.01$, and $***P < 0.001$.

ASP (C3 KO) or C5L2 signaling display increased energy expenditure.

The present study directly addresses the mechanism underlying this altered energy expenditure. We observed, through examination of the glycolytic and fatty acid oxidation pathways in the muscle, that mice lacking a functional ASP-C5L2 pathway (C3 KO) have increased energy expenditure through increased oxygen consumption and display a preference for fatty acids as a substrate over carbohydrates. The shift is indicated by increased fatty acid oxidation, higher CD36 content, and increased HADH activity. Decrease in glucose oxidation capacities and activities of glycolytic enzymes further supports the substrate preference.

The mechanism of increased fatty acid oxidation in the muscle of C3 KO mice may derive from an increased diversion of substrate (fatty acids) away from adipose tissue and toward muscle. Our previous work showed that the C3 KO mice had excess circulating lipid availability associated with delayed postprandial TG and NEFA clearance (24, 25, 39). The effect of substrate availability on oxidation is supported by recent data in C57BL/6 mice, *db/db* mice, and obese rats showing that excess lipid availability due to a HF diet resulted in increased *ex vivo* muscle fatty acid oxidation and activation of major β -oxidation enzymes (35). The increased lipid accessibility was also associated with impaired glucose clearance as well as impaired insulin action (35).

The increased fatty acid muscle metabolism in C3 KO mice may be substrate driven (as discussed above), resulting in a corresponding decrease activity in the glycolytic pathway. The increase in fasting glucose, with a trend for increased insulin, would also be consistent with an overload of fat to the muscle, leading to insulin resistance. In the present study, *ex vivo* glucose oxidation was decreased, glucose clearance was delayed, glycogen reserves were decreased, and phosphofructose kinase activity was downregulated. All of these are consistent with the inhibitory effect of increased fatty acid oxidation on the glycolytic pathway, detailed a number of years ago as the Randle cycle, which states that substrate competition is dominated by fatty acids, which can inhibit (via citrate accumulation) glycolysis (31). HF diet consumption has also been shown to reduce muscle glycogen levels (17). Furthermore, the switch in metabolic substrate has been well described in studies on fasting and exercise, which have shown a profound preference toward fatty acid utilization due to diminished glucose availability (5).

Substrate diversion and alterations in muscle metabolism have also been identified in a number of other mouse knockout models. Acetyl-CoA carboxylase-2-deficient mice (ACC2 KO) and stearoyl-CoA desaturase-1-deficient mice (SCD1 KO) are two examples of KO mice that show many similar characteristics (although not all) to the C3 KO and C5L2 KO mice. In both cases, the mice have a lean phenotype with enhanced fatty acid oxidation and increased metabolic rate coupled to increased food intake (1, 6, 7, 26). On average, SCD1 KO mice consume 25% more food than their WT counterparts without accumulating fat, thus making them resistant to diet-induced obesity. SCD1 KO mice have higher rates of oxygen consumption, and genes involved in β -oxidation were shown to be upregulated (7). One striking difference between ACC2 KO and SCD1 KO mice and the C3 KO mice is the increase in AMPK activity related to the elevated energy expenditure.

C3 KO mice display reduced AMPK activity in both skeletal and cardiac muscle on a HF diet. AMPK is commonly referred to as the cell's fuel regulator, sensing disturbances in energy requirements (ATP/AMP) (15). In response to low cellular ATP, AMPK activates both fatty acid oxidative and glycolytic enzymes to replenish energy stores while downregulating anabolic pathways such as fatty acid synthesis (15). AMPK is highly regulated by a number of hormones, physiological conditions, and pharmacological agents. Studies have shown that skeletal muscle AMPK is downregulated in trained rats during acute exercise, with age, and HF diet consumption (9, 20, 32). Recently, Wu et al. (37) demonstrated that chronic palmitate exposure inhibited endothelial AMPK phosphorylation and activity. Therefore, the elevated postprandial plasma NEFA observed in C3 KO mice (23, 24, 39) could contribute, by the pathway described above, to the reduced AMPK activities observed in the present study.

On the other hand, the higher energy expenditure in C3 KO mice could be attributed to a direct lack of ASP-C5L2 signaling in the muscle. C5L2 is highly expressed in muscle tissue (Ref. 27 and Roy C, personal observation), and ASP has been shown to stimulate glucose transport in muscle L6 cells (34). Both C3 KO and C5L2 KO mice demonstrate delayed glucose clearance after a challenge with a glucose tolerance test (28). Therefore, a lack of ASP stimulation of muscle glucose uptake (and increased fatty acid availability due to inefficient adipose storage) may drive the enhanced lipid oxidation. This is supported by the results obtained when hyperphagia in the C3 KO mice is controlled, where C3 KO mice body weight is lower than that of their WT counterparts.

The importance of the ASP-C5L2 pathway is highlighted in its regulation of fatty acid metabolism. Inhibition of the pathway leads to excess plasma lipid availability that increases mitochondrial β -oxidation capacity in muscle and overall energy expenditure. On the other hand, an increase in plasma fatty acids, particularly in humans, may lead to undesirable effects (i.e., inducing insulin resistance). One of the most salient concerns with delaying dietary lipid clearance is the potential for increased TG delivery to the liver leading to increased lipoprotein production, which is a risk for metabolic syndrome (30). The increased food intake noted in the C3 KO mice may also be an undesirable side effect when blockage of ASP-C5L2 as a potential obesity target is considered. Further studies are necessary to determine the outcome of both acute and chronic ASP-C5L2 blocking in obese mouse models to provide better data on how these side effects may be mitigated.

GRANTS

This study was supported by a grant from the Canadian Institutes of Health Research (MOP-77532 to K. Cianflone). K. Cianflone holds a Canada Research Chair in Adipose Tissue.

REFERENCES

1. Abu-Elheiga L, Matzuk MM, Abo-Hashema KA, Wakil SJ. Continuous fatty acid oxidation and reduced fat storage in mice lacking acetyl-CoA carboxylase 2. *Science* 291: 2613–2616, 2001.
2. Brown RP, Delp MD, Lindstedt SL, Rhomberg LR, Beliles RP. Physiological parameter values for physiologically based pharmacokinetic models. *Toxicol Ind Health* 13: 407–484, 1997.
3. Cannon B, Nedergaard J. Brown adipose tissue: function and physiological significance. *Physiol Rev* 84: 277–359, 2004.

4. Cianflone K, Xia Z, Chen LY. Critical review of acylation stimulating protein physiology in humans and rodents. *Biochim Biophys Acta* 1609: 127–143, 2003.
5. de Lange P, Moreno M, Silvestri E, Lombardi A, Goglia F, Lanni A. Fuel economy in food-deprived skeletal muscle: signaling pathways and regulatory mechanisms. *FASEB J* 21: 3431–3441, 2007.
6. Dobrzyn A, Dobrzyn P, Lee SH, Miyazaki M, Cohen P, Asilmaz E, Hardie DG, Friedman JM, Ntambi JM. Stearoyl-CoA desaturase-1 deficiency reduces ceramide synthesis by downregulating serine palmitoyltransferase and increasing β -oxidation in skeletal muscle. *Am J Physiol Endocrinol Metab* 288: E599–E607, 2005.
7. Dobrzyn A, Ntambi JM. The role of stearoyl-CoA desaturase in body weight regulation. *Trends Cardiovasc Med* 14: 77–81, 2004.
8. Doucet E, Tremblay A, Simoneau JA, Joanisse DR. Skeletal muscle enzymes as predictors of 24-h energy metabolism in reduced-obese persons. *Am J Clin Nutr* 78: 430–435, 2003.
9. Durante PE, Mustard KJ, Park SH, Winder WW, Hardie DG. Effects of endurance training on activity and expression of AMP-activated protein kinase isoforms in rat muscles. *Am J Physiol Endocrinol Metab* 283: E178–E186, 2002.
10. Faraj M, Cianflone K. Differential regulation of fatty acid trapping in mouse adipose tissue and muscle by ASP. *Am J Physiol Endocrinol Metab* 287: E150–E159, 2004.
11. Faraj M, Sniderman AD, Cianflone K. ASP enhances in situ lipoprotein lipase activity by increasing fatty acid trapping in adipocytes. *J Lipid Res* 45: 657–666, 2004.
12. Gauthier JM, Theriault R, Theriault G, Gelinas Y, Simoneau JA. Electrical stimulation-induced changes in skeletal muscle enzymes of men and women. *Med Sci Sports Exerc* 24: 1252–1256, 1992.
13. Gayles EC, Pagliassotti MJ, Prach PA, Koppenhafer TA, Hill JO. Contribution of energy intake and tissue enzymatic profile to body weight gain in high-fat-fed rats. *Am J Physiol Regul Integr Comp Physiol* 272: R188–R194, 1997.
14. Germinario R, Sniderman AD, Manuel S, Lefebvre SP, Baldo A, Cianflone K. Coordinate regulation of triacylglycerol synthesis and glucose transport by acylation-stimulating protein. *Metabolism* 42: 574–580, 1993.
15. Hawley SA, Davison M, Woods A, Davies SP, Beri RK, Carling D, Hardie DG. Characterization of the AMP-activated protein kinase kinase from rat liver and identification of threonine 172 as the major site at which it phosphorylates AMP-activated protein kinase. *J Biol Chem* 271: 27879–27887, 1996.
16. Hesselink MK, Kuipers H, Keizer HA, Drost MR, van der Vusse GJ. Acute and sustained effects of isometric and lengthening muscle contractions on high-energy phosphates and glycogen metabolism in rat tibialis anterior muscle. *J Muscle Res Cell Motil* 19: 373–380, 1998.
17. Huang X, Hansson M, Laurila E, Ahren B, Groop L. Fat feeding impairs glycogen synthase activity in mice without effects on its gene expression. *Metabolism* 52: 535–539, 2003.
18. Kalant D, Cain SA, Maslowska M, Sniderman AD, Cianflone K, Monk PN. The chemoattractant receptor-like protein C5L2 binds the C3a des-Arg77/acylation-stimulating protein. *J Biol Chem* 278: 11123–11129, 2003.
19. Kalant D, Maclaren R, Cui W, Samanta R, Monk PN, Laporte SA, Cianflone K. C5L2 is a functional receptor for acylation stimulating protein. *J Biol Chem* 280: 23936–23944, 2005.
20. Liu Y, Wan Q, Guan Q, Gao L, Zhao J. High-fat diet feeding impairs both the expression and activity of AMPK α in rats' skeletal muscle. *Biochem Biophys Res Commun* 339: 701–707, 2006.
21. Maslowska M, Sniderman AD, Germinario R, Cianflone K. ASP stimulates glucose transport in cultured human adipocytes. *Int J Obes Relat Metab Disord* 21: 261–266, 1997.
22. Murray I, Havel PJ, Sniderman AD, Cianflone K. Reduced body weight, adipose tissue, and leptin levels despite increased energy intake in female mice lacking acylation-stimulating protein. *Endocrinology* 141: 1041–1049, 2000.
23. Murray I, Sniderman AD, Cianflone K. Enhanced triglyceride clearance with intraperitoneal human acylation stimulating protein in C57BL/6 mice. *Am J Physiol Endocrinol Metab* 277: E474–E480, 1999.
24. Murray I, Sniderman AD, Cianflone K. Mice lacking acylation stimulating protein (ASP) have delayed postprandial triglyceride clearance. *J Lipid Res* 40: 1671–1676, 1999.
25. Murray I, Sniderman AD, Havel PJ, Cianflone K. Acylation stimulating protein (ASP) deficiency alters postprandial and adipose tissue metabolism in male mice. *J Biol Chem* 274: 36219–36225, 1999.
26. Oh W, Abu-Elheiga L, Kordari P, Gu Z, Shaikenov T, Chirala SS, Wakil SJ. Glucose and fat metabolism in adipose tissue of acetyl-CoA carboxylase 2 knockout mice. *Proc Natl Acad Sci USA* 102: 1384–1389, 2005.
27. Okinaka S, Slattery D, Humbles A, Zsengeller Z, Morteau O, Kinrade MB, Brodbeck RM, Krause JE, Choe HR, Gerard NP, Gerard C. C5L2, a nonsignaling C5A binding protein. *Biochemistry* 42: 9406–9415, 2003.
28. Pagliarunga S, Schrauwen P, Roy C, Moonen-Kornips E, Lu H, Hesselink MK, Deshaies Y, Richard D, Cianflone K. Reduced adipose tissue triglyceride synthesis and increased muscle fatty acid oxidation in C5L2 knockout mice. *J Endocrinol* 194: 293–304, 2007.
29. Pekna M, Hietala MA, Rosklint T, Betsholtz C, Pekny M. Targeted disruption of the murine gene coding for the third complement component (C3). *Scand J Immunol* 47: 25–29, 1998.
30. Petruzzelli M, Lo Sasso G, Portincasa P, Palasciano G, Moschetta A. Targeting the liver in the metabolic syndrome: evidence from animal models. *Curr Pharm Des* 13: 2199–2207, 2007.
31. Randle PJ. Regulatory interactions between lipids and carbohydrates: the glucose fatty acid cycle after 35 years. *Diabetes Metab Rev* 14: 263–283, 1998.
32. Reznick RM, Zong H, Li J, Morino K, Moore IK, Yu HJ, Liu ZX, Dong J, Mustard KJ, Hawley SA, Befroy D, Pypaert M, Hardie DG, Young LH, Shulman GI. Aging-associated reductions in AMP-activated protein kinase activity and mitochondrial biogenesis. *Cell Metab* 5: 151–156, 2007.
33. Sambandam N, Steinmetz M, Chu A, Altarejos JY, Dyck JR, Lopaschuk GD. Malonyl-CoA decarboxylase (MCD) is differentially regulated in subcellular compartments by 5'AMP-activated protein kinase (AMPK). Studies using H9c2 cells overexpressing MCD and AMPK by adenoviral gene transfer technique. *Eur J Biochem* 271: 2831–2840, 2004.
34. Tao Y, Cianflone K, Sniderman AD, Colby-Germinario SP, Germinario RJ. Acylation-stimulating protein (ASP) regulates glucose transport in the rat L6 muscle cell line. *Biochim Biophys Acta* 1344: 221–229, 1997.
35. Turner N, Bruce CR, Beale SM, Hoehn KL, So T, Rolph MS, Cooney GJ. Excess lipid availability increases mitochondrial fatty acid oxidative capacity in muscle: evidence against a role for reduced fatty acid oxidation in lipid-induced insulin resistance in rodents. *Diabetes* 56: 2085–2092, 2007.
36. Van Harmelen V, Reynisdottir S, Cianflone K, Degerman E, Hoffstedt J, Nilsell K, Sniderman A, Arner P. Mechanisms involved in the regulation of free fatty acid release from isolated human fat cells by acylation-stimulating protein and insulin. *J Biol Chem* 274: 18243–18251, 1999.
37. Wu Y, Song P, Xu J, Zhang M, Zou MH. Activation of protein phosphatase 2A by palmitate inhibits AMP-activated protein kinase. *J Biol Chem* 282: 9777–9788, 2007.
38. Xia Z, Sniderman AD, Cianflone K. Acylation-stimulating protein (ASP) deficiency induces obesity resistance and increased energy expenditure in *ob/ob* mice. *J Biol Chem* 277: 45874–45879, 2002.
39. Xia Z, Stanhope KL, Digitale E, Simion OM, Chen L, Havel P, Cianflone K. Acylation-stimulating protein (ASP)/complement C3adesArg deficiency results in increased energy expenditure in mice. *J Biol Chem* 279: 4051–4057, 2004.
40. Yasruel Z, Cianflone K, Sniderman AD, Rosenbloom M, Walsh M, Rodriguez MA. Effect of acylation stimulating protein on the triacylglycerol synthetic pathway of human adipose tissue. *Lipids* 26: 495–499, 1991.